NeuroImage: Clinical 28 (2020) 102390

Contents lists available at ScienceDirect

NeuroImage: Clinical

journal homepage: www.elsevier.com/locate/ynicl

Inter-channel phase differences during sleep spindles are altered in Veterans with PTSD

Chao Wang[a,b], Srinivas Laxminarayan[a,b], J. David Cashmere[c], Anne Germain[c], Jaques Reifman[a,*]

[a] Department of Defense Biotechnology High Performance Computing Software Applications Institute, Telemedicine and Advanced Technology Research Center, United States Army Medical Research and Development Command, USA
[b] The Henry M. Jackson Foundation for the Advancement of Military Medicine, Inc., USA
[c] Department of Psychiatry, University of Pittsburgh School of Medicine, USA

ARTICLE INFO

Keywords:
Post-traumatic stress disorder
Combat-exposed Veteran
Sleep spindles
Synchronization
Phase-locking value
Phase difference
High-density EEG
Reproducibility

ABSTRACT

Sleep disturbances are common complaints in patients with post-traumatic stress disorder (PTSD). To date, however, objective markers of PTSD during sleep remain elusive. Sleep spindles are distinctive bursts of brain oscillatory activity during non-rapid eye movement (NREM) sleep and have been implicated in sleep protection and sleep-dependent memory processes. In healthy sleep, spindles observed in electroencephalogram (EEG) data are highly synchronized across different regions of the scalp. Here, we aimed to investigate whether the spatiotemporal synchronization patterns between EEG channels during sleep spindles, as quantified by the phase-locking value (PLV) and the mean phase difference (MPD), are altered in PTSD. Using high-density (64-channel) EEG data recorded from 78 combat-exposed Veteran men (31 with PTSD and 47 without PTSD) during two consecutive nights of sleep, we examined group differences in the PLV and MPD for slow (10–13 Hz) and fast (13–16 Hz) spindles separately. To evaluate the reproducibility of our findings, we set apart the first 47 consecutive participants (18 with PTSD) for the initial discovery and reserved the remaining 31 participants (13 with PTSD) for replication analysis. In the discovery analysis, compared to the non-PTSD group, the PTSD group showed smaller MPDs during slow spindles between the frontal and centro-parietal channel pairs on both nights. We obtained reproducible results in the replication analysis in terms of statistical significance and effect size. The PLVs during slow or fast spindles did not significantly differ between groups. The reduced inter-channel phase difference during slow spindles in PTSD may reflect pathological changes in the underlying thalamocortical circuits. This novel finding, if independently validated, may prove useful in developing sleep-focused PTSD diagnostics and interventions.

1. Introduction

Individuals with post-traumatic stress disorder (PTSD) often suffer from sleep disturbances, such as trouble falling or maintaining sleep and recurrent nightmares (Mellman and Hipolito, 2006; Neylan et al., 1998). Although the prevalence rates of self-reported sleep problems in PTSD have been documented to be as high as 90% (Neylan et al., 1998), the results of polysomnography (PSG) studies examining objective measures of sleep in PTSD have been inconsistent [see Kobayashi et al. (2007) and Germain (2013) for reviews]. The lack of reliable sleep markers of PTSD presents an obstacle to understanding the pathophysiology of its associated sleep symptoms and to developing sleep-specific diagnostics and interventions for the disorder. To bridge this gap, we have made several attempts to identify brain activity changes in PTSD during sleep that are reproducible, by examining features of electroencephalogram (EEG) spectral power (Wang et al., 2020a), EEG synchrony (Laxminarayan et al., 2020), and sleep spindles (Wang et al., 2020b). In particular, sleep spindles are signature neural events during non-rapid eye movement (NREM) sleep that are thought to play key roles in sleep-dependent memory consolidation (Fogel and Smith, 2011) and sleep protection (Astori et al., 2013; Luthi, 2014). In a recent study, we made an initial effort to investigate whether sleep spindle characteristics (i.e., amplitude, duration, oscillatory frequency, and density) are altered in subjects with PTSD compared to those without PTSD (Wang et al., 2020b). Although spindle amplitude, duration, and density did not differ between the two groups, the oscillatory frequencies of sleep spindles were higher in PTSD subjects than in non-PTSD subjects, with consistent trends across nights and subsamples of

* Corresponding author: Department of Defense Biotechnology High Performance Computing Software Applications Institute, Telemedicine and Advanced Technology Research Center, U.S. Army Medical Research and Development Command, ATTN: FCMR-TT, 504 Scott Street, Fort Detrick, MD 21702, USA.
E-mail address: jaques.reifman.civ@mail.mil (J. Reifman).

https://doi.org/10.1016/j.nicl.2020.102390
Received 6 May 2020; Received in revised form 30 June 2020; Accepted 17 August 2020
Available online 20 August 2020

the study population.

Another important aspect of sleep spindles that may be altered in PTSD is their spatiotemporal dynamics. Spindles are highly synchronous events that occur across different regions of the scalp (Bonjean et al., 2012; Contreras et al., 1997). Although they arise from thalamic circuits, corticothalamic feedback projections and divergent connectivity between thalamic and cortical neurons are essential for establishing the long-range synchronization of spindles (Beenhakker and Huguenard, 2009; Contreras et al., 1997). Evidence suggests that thalamic dysfunction is partly involved in the etiology of PTSD (Kim et al., 2007; Lanius et al., 2006; Suarez-Jimenez et al., 2019). Moreover, the functional connectivity between the thalamus and cortical regions has been shown to be altered in PTSD during script-driven imagery (Lanius et al., 2005) and in the resting state (Terpou et al., 2018; Yin et al., 2011). It is therefore reasonable to suspect that thalamocortical connectivity is also disrupted during sleep in PTSD, and that this disruption may lead to aberrant spatiotemporal patterns of sleep spindles. This possibility, however, has not been examined in previous studies. Here, we hypothesize that the spatiotemporal synchronization patterns of spindles may discriminate individuals with and without PTSD.

One way to assess the synchrony of sleep spindles is by examining two indices that characterize the phase relations between spindles recorded at spatially separated EEG channels: the phase-locking value (PLV) (Lachaux et al., 1999) and the mean phase difference (MPD) (Thatcher, 2012; Thatcher et al., 2008). The PLV, which estimates the stability of the phase difference between two signals, is a commonly used index for quantifying phase synchronization (Aydore et al., 2013). A large PLV between EEG signals indicates stable phase relations among the underlying neuronal groups and, hence, suggests strong functional neural connectivity (Varela et al., 2001). The MPD, which complements the PLV, measures the average phase lead or lag between two coupled signals. A non-zero MPD between EEG signals suggests a delay of information transmission in the underlying neural system (Thatcher, 2012). Given that reciprocal interactions between thalamic and cortical neurons are responsible for generating and synchronizing spindle oscillations (Beenhakker and Huguenard, 2009; Luthi, 2014), the PLV and MPD during spindles are likely to reflect the coupling strength and coupling delay, respectively, of the underlying thalamocortical network.

The aim of the present work was to investigate whether the spatiotemporal dynamics of spindles, as quantified by the PLV and the MPD, are altered in individuals with PTSD. To this end, we analyzed high-density (64-channel) EEG data recorded from 78 combat-exposed Veteran men with (n = 31) and without (n = 47) PTSD during two consecutive nights of sleep. After detecting sleep spindles using an automatic algorithm, we conducted PLV and MPD analyses on data from both nights. We analyzed slow (10–13 Hz) and fast (13–16 Hz) spindles separately, because these two types of spindles are distributed distinctly across brain regions (Andrillon et al., 2011). To assess the reproducibility of our findings, we used the first 47 consecutive participants (18 with PTSD) for the initial discovery, and performed replication analyses using the remaining 31 participants (13 with PTSD) to examine whether we could reproduce the initial findings.

2. Materials and methods

2.1. Participants

Eighty-five post-9/11 Veterans who had been deployed in support of the global war on terror completed the screening and experimental procedures. Thirty-seven were diagnosed with PTSD (31 men and 6 women) and 48 without PTSD (47 men and 1 woman). All participants were between the ages of 18 and 50 years and free of medications known to affect sleep or daytime functioning for at least 2 weeks (6 weeks for fluoxetine). We excluded participants who had *1*) current or untreated severe depression, *2*) a history of psychotic or bipolar disorder, *3*) alcohol or substance dependence within the past 3 months, *4*) current post-concussive symptoms or rehabilitation treatment for traumatic brain injury, *5*) a significant or unstable acute or chronic medical condition, *6*) a current sleep disorder other than insomnia or nightmares, such as obstructive sleep apnea, restless leg syndrome, delayed sleep phase syndrome, narcolepsy, and periodic leg movement disorder, or a current night-shift work schedule, *7*) more than 2 cups of coffee (or the equivalent amount of caffeine) per day on average, or *8*) alcohol use of more than 2 alcoholic drinks per day (or more than 14 drinks per week) on average. The study protocol was approved by the University of Pittsburgh Institutional Review Board (Pittsburgh, PA) and by the U.S. Army Medical Research and Development Command's Human Research Protection Office (Ft. Detrick, MD). All participants provided written informed consent prior to the screening process.

We used the Clinician-Administered PTSD Scale (CAPS) (Blake et al., 1995) and the Structured Clinical Interview for Sleep Disorders (Buysse et al., 2011) to assess the presence of PTSD and Diagnostic and Statistical Manual of Mental Disorders IV (DSM-IV) sleep disorders, respectively, with a physician making the PTSD diagnosis. Other clinical assessments included the Patient Health Questionnaire-9 (PHQ-9) (Lowe et al., 2004) to assess depression, the Pittsburgh Sleep Quality Index (PSQI) (Buysse et al., 1989) and the Insomnia Severity Index (ISI) (Bastien et al., 2001) to assess sleep, the Epworth Sleepiness Scale (ESS) (Johns, 1991) to assess daytime sleepiness, and the Structured Clinical Interview for DSM-IV Axis I Disorders (First and Spitzer, 1997) to assess the presence of mood, anxiety, psychosis, alcohol use, and substance use disorders. We used a 2-week medication history questionnaire to verify that the amounts of caffeine and alcohol consumption were within the permissible thresholds. To monitor habitual sleep, we asked participants to complete a sleep diary for 10 consecutive days prior to the laboratory study. To screen for sleep apnea, we asked participants to wear a portable apnea screening device (ApneaLink; ResMed Corp., San Diego, CA) at home for one night prior to arrival at the laboratory.

The experiment involved two consecutive nights and days of laboratory stay, which began at 20:00 on Night 1. For each night, we provided participants with the opportunity to sleep 8 h (23:00–07:00) and recorded high-density EEG data throughout the entire night of sleep using a 64-channel HydroCel Geodesic Sensor Net (Electrical Geodesics Inc., Eugene, OR). During the day, participants performed multiple sessions of alertness and working-memory tests. The procedures conducted on Night 1 and Day 1 were the same as those conducted on Night 2 and Day 2.

Because there were 6 women in the PTSD group but only 1 woman in the non-PTSD group, we restricted our analyses to the 78 men to eliminate potential effects due to an imbalance in the sex ratio. To assess the reproducibility of our findings, we used the first 47 consecutive participants (~60% of the total, 18 with PTSD) for the initial discovery, and reserved the remaining 31 participants (~40% of the total, 13 with PTSD) for the replication assessment.

The sample used in the present study was the same as that used in our previous work, in which we reported the clinical characteristics and sleep architecture parameters of the participants (Laxminarayan et al., 2020; Wang et al., 2020a, 2020b). Briefly, PTSD and non-PTSD participants did not differ significantly with respect to age or the Apnea-Hypopnea Index (AHI) in both the discovery and replication sets ($p > 0.05$). The PTSD group had higher CAPS, PSQI, ISI, and PHQ-9 scores than did the non-PTSD group in both data sets (all p-values < 0.001). The ESS score was higher in PTSD participants than in non-PTSD participants in the discovery set ($p = 0.003$) but not in the replication set ($p = 0.856$). With respect to sleep architecture parameters, no group differences were consistent across nights and subsamples. We provide detailed information in Supplementary Tables S1 and S2.

2.2. Recording and preprocessing of sleep EEG data, and detection of sleep spindles

We recorded 64-channel EEG data at 250 Hz during each of the two nights of the study, using the linked mastoids as the reference. We visually scored sleep stages in 30-s epochs for each night according to the American Academy of Sleep Medicine standards. The EEG preprocessing and spindle detection methods were as previously described (Wang et al., 2020b). Briefly, we segmented the data into 5-s epochs and used previously validated algorithms (Brunner et al., 1996; Doman et al., 1995; Liu et al., 2018) to remove all epochs contaminated by muscle and ocular artifacts. Regarding spindle detection, we considered spindles falling within the 10–13 Hz frequency range as slow spindles, while considering those falling in the 13–16 Hz range as fast spindles. To detect slow and fast spindles, we first band-pass filtered the raw EEG signals for the artifact-free epochs corresponding to N2 and N3 stages of NREM sleep in the frequency ranges of slow spindles (10–13 Hz) and fast spindles (13–16 Hz) separately. Then, we calculated the root mean square (RMS) of the filtered signal over a 250-ms sliding window with a 25-ms step size. Finally, we established sleep-spindle time intervals by retaining segments where the amplitude of the RMS signal exceeded its 95th percentile value for at least 0.5 s but no more than 3.0 s (Martin et al., 2013; Warby et al., 2014). We detected slow and fast spindles separately for each EEG channel.

2.3. Estimation of PLV and MPD during sleep spindles

Fig. 1 shows our procedure for estimating the PLV and MPD for a pair of EEG channels. First, we arbitrarily designated one channel as the reference and considered the spindle time intervals detected from it as the reference time windows for analysis. Next, we extracted the instantaneous phase of the filtered signals within the analysis windows for the reference channel and for the corresponding time segments of the other channel using the Hilbert transform (Rosenblum and Kurths, 1998). Then, we obtained the instantaneous phase difference $\Delta\varphi$ at each time point m, with $m = 1, 2, \cdots, M$, at a 250-Hz sampling rate, by calculating the phase difference between the two channels. Note that M denotes the total number of time points of all analysis windows. Finally, we projected the instantaneous phase differences of all M time points onto the unit circle and estimated the PLV as the length of the mean resultant vector $\vec{r}$ of the instantaneous phase differences:

$$\mathrm{PLV} = ||\vec{r}|| = |\frac{1}{M}\sum_{m=1}^{M} e^{i\Delta\varphi(m)}| \quad (1)$$

The PLV ranges from 0 to 1, where 1 indicates a constant phase difference over time (i.e., a perfect phase synchronization) and 0 indicates a random phase difference (i.e., no phase synchronization). Note that the PLV indicates the stability of the phase difference over time (i.e., the strength of synchronization) independent of its magnitude (e.g., whether it is 0 or 90°).

To quantify the average phase lead or lag between two channels, we estimated the MPD by calculating the angle θ of the mean resultant vector $\vec{r}$ (i.e., the circular mean) of the instantaneous phase differences:

$$\mathrm{MPD} = \theta = angle(\vec{r}) = \arg\left(\sum_{m=1}^{M} e^{i\Delta\varphi(m)}\right) \quad (2)$$

We analyzed the PLV and the MPD for slow and fast spindles separately. Instead of testing all possible pairs of EEG channels, we selected one channel each for slow and fast spindles as the "seed channel" (reference) and investigated the phase relations of this reference signal to the signals at each of the other 63 channels. In this way, we assessed the PLV and MPD topographically and reduced the number of multiple comparisons to prevent spurious findings. Because slow spindles are most prominent in the frontal region and fast spindles are most prominent in the centro-parietal region (Cox et al., 2017; Lustenberger et al., 2015), we selected the frontal channel Fz and parietal channel Pz as the seed channels for the slow- and fast-spindle analyses, respectively, as illustrated by the "stars" in Fig. 2. We considered the spindle intervals detected from the seed channels as the reference time windows for analysis, and estimated the PLV and MPD by averaging the instantaneous phase differences across all spindle time intervals. Note that if the distribution of instantaneous phase differences were dispersed on the unit circle (as indicated by a small PLV), the MPD would be a poor representation of the data. Therefore, we only analyzed the MPD for channel pairs with a mean PLV greater than 0.5 across all participants. To avoid potential age effects, we performed a regression-based age correction on the PLV and MPD measures using a procedure described previously (Wang et al., 2020a). We conduced our analyses with MATLAB software (The MathWorks Inc., Natick, MA), using the CircStat (Berens, 2009) and EEGLAB (Delorme and Makeig, 2004) toolboxes.

2.4. Statistical analyses

We used the Wilcoxon rank-sum test (evaluated by the Z-statistic) and the Watson − Williams test (an analog of the two-sample *t*-test for use with circular data, evaluated by the F- statistic) to assess group differences in PLV and MPD, respectively. To correct for multiple comparisons across channel pairs, we performed a permutation test using the maximum-statistic approach (Nichols and Holmes, 2002). Briefly, we permuted the datasets 10,000 times by randomly re-labeling the group labels (PTSD and non-PTSD) of the original data. Next, for each permutation, we selected the channel pair with the maximum test statistic and, offer the 10,000 permutations, formed a distribution. Then, we assessed the significance (i.e., the *p*-values) of the group differences by comparing the test statistics of the original (correctly labeled) data to this empirical distribution. To further account for multiple comparisons across the four metrics investigated (i.e., PLV and MPD for slow and fast spindles), we performed Bonferroni corrections. To examine group differences for different sleep cycles, we conducted 2-way repeated measures analyses of variance (rANOVA) with group (PTSD or non-PTSD) as the between-subject factor and sleep cycle (1, 2, or 3) as the within-subject factor, while using the Greenhouse-Geisser correction when the data violated sphericity assumptions (based on the Mauchly's test of sphericity). We considered p-values < 0.05 to be statistically significant.

2.5. Evaluation of reproducibility

No single test can sufficiently describe whether a replication is a success or a failure (Open Science, 2015). Thus, we evaluated the reproducibility of our findings based on three tests, as described previously (Wang et al., 2020a). Briefly, the first test evaluated whether the replication *p*-values were significant ($p < 0.05$) and in the same direction as the original *p*-values. The second test evaluated whether the replication effect sizes fell within the 95% confidence interval (CI) of the original effect sizes, and the third test evaluated whether the findings remained significant ($p < 0.05$) after combining the discovery and replication subsamples. We quantified the effect size using Cohen's *d*, which is calculated as the difference between the means of the two groups (PTSD minus non-PTSD) divided by the pooled standard deviation. We used the circular mean and the circular standard deviation when computing Cohen's *d* for the findings on the MPD.

3. Results

3.1. Number of sleep spindles detected in the discovery and replication sets

Table 1 shows the number of slow and fast spindles for the PTSD and non-PTSD groups during the whole night of sleep as well as during

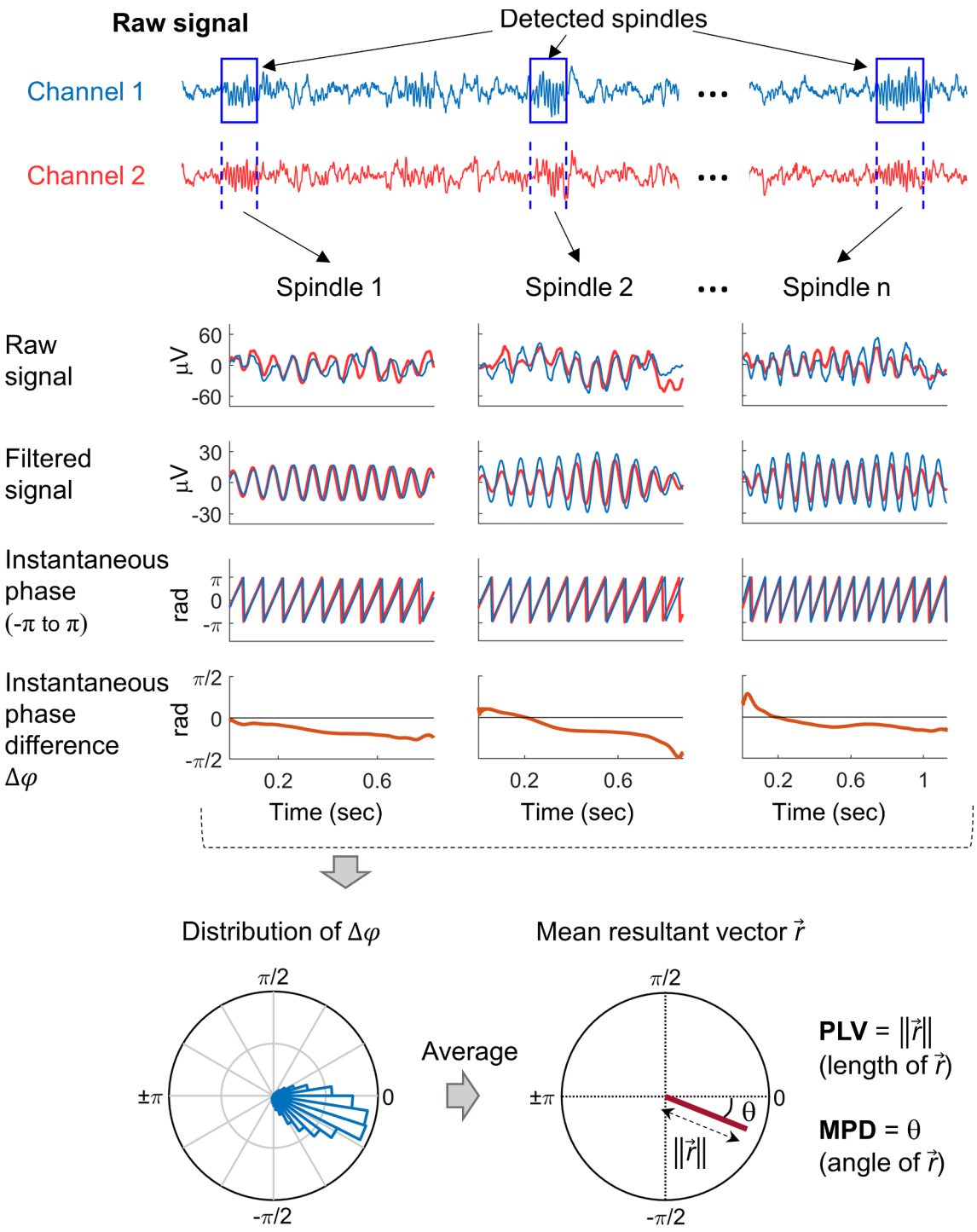

Fig. 1. Procedure for estimating the phase-locking value (an index of phase synchronization) and the mean phase difference between sleep spindles from a pair of EEG channels.

each of the first 3 sleep cycles. A 2-way rANOVA test with group and sleep cycle as between- and within-subject factors, respectively, revealed no significant effect of group on the number of slow or fast spindles for either the discovery or the replication set (all p-values $>$ 0.05, Supplementary Table S3). The effect of sleep cycle on the number of spindles was significant in some, but not all tests involving different spindle types, nights, and subsamples (see Supplementary Table S3).

When comparing the discovery set versus the replication set, their differences in the number of slow spindles (whole-night measure) were significant for the non-PTSD group ($p < 0.05$ on both nights, Wilcoxon rank-sum test), but were not significant for the PTSD group ($p > 0.05$ on both nights); the differences in the number of fast spindles (whole-night measure) between the discovery and replication sets were not significant for either the PTSD group or the non-PTSD group (all p-values > 0.05).

3.2. Topographical analysis of PLV and MPD during sleep spindles (discovery analysis)

3.2.1. Results for slow spindles

Fig. 2A shows the topographical distributions of the PLV between the frontal seed channel Fz and all other channels for slow spindles. In

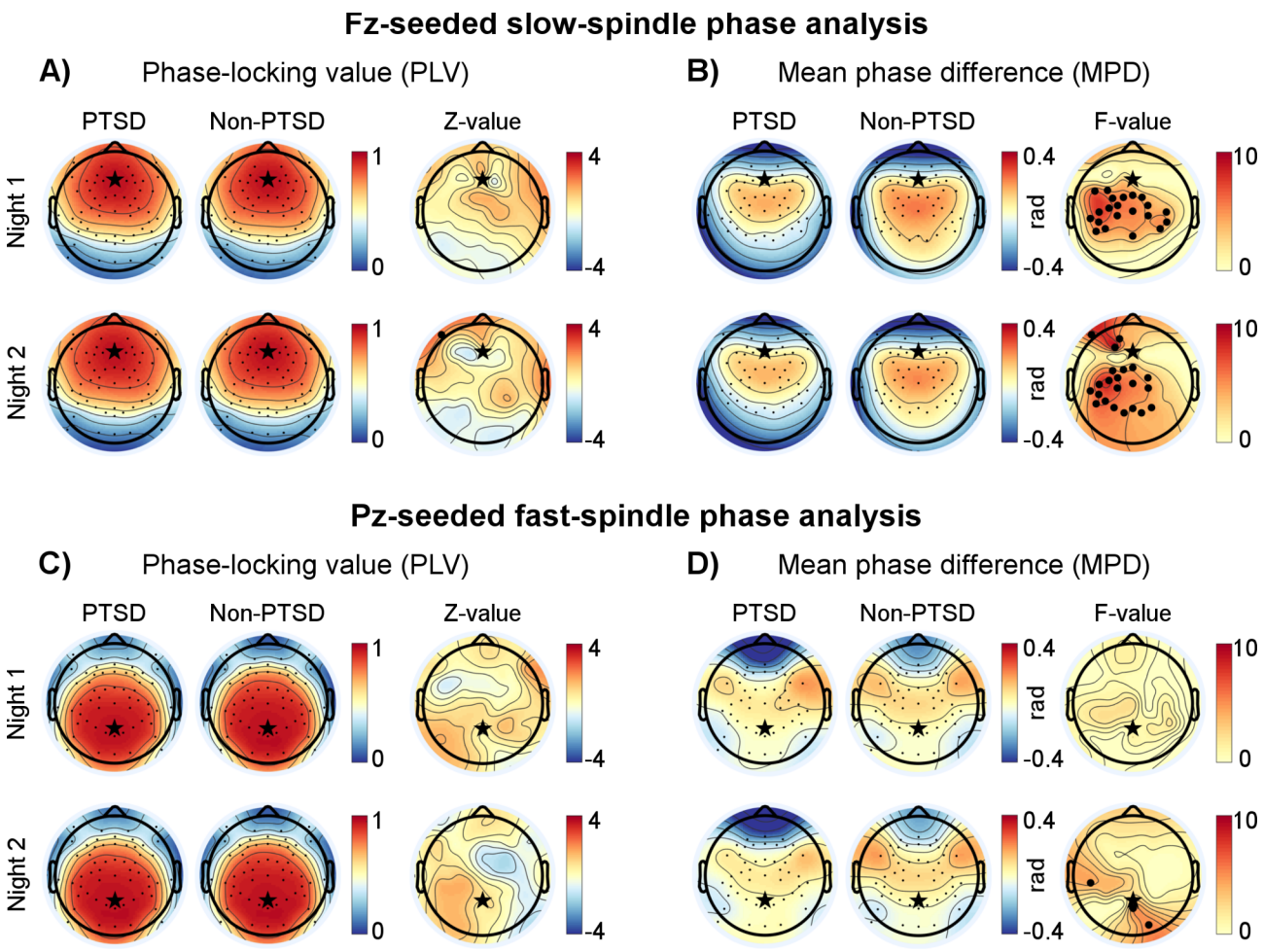

Fig. 2. Topographical results of the phase-locking value (PLV) and the mean phase difference (MPD) during slow and fast spindles for the discovery analysis (18 PTSD and 29 non-PTSD). Black stars indicate the two "seed channels" (Fz in the frontal region and Pz in the parietal region) used in the pair-wise analyses. A) Results of the PLV during slow spindles using Fz as the seed channel. The first and second columns show the PLV values of the 63 pair-wise analyses for the PTSD and non-PTSD groups, respectively, while the third column shows the Z-values of the statistical comparisons (Wilcoxon rank-sum tests) between the two groups at individual channels. Small black dots denote the individual channels. B) Results of the MPD during slow spindles using Fz as the seed channel. The first and second columns show the MPD values of the 63 pair-wise analyses for the PTSD and non-PTSD groups, respectively, whereas the third column shows F-values of the statistical comparisons (Watson − Williams tests) between the two groups at individual channels. Small black dots denote the individual channels for which the PLV was greater than 0.5 when referenced to Fz, whereas large black dots indicate channels with uncorrected *p*-values less than 0.05. C) Results of the PLV during fast spindles using Pz as the seed channel. D) Results of the MPD during fast spindles using Pz as the seed channel.

both the PTSD (n = 18; Fig. 2A, first column) and non-PTSD (n = 29; Fig. 2A, second column) groups, the PLV was greater than 0.5 for most of the frontal and parietal channels, indicating strong phase synchronization with the seed channel. A comparison between the PTSD and non-PTSD groups revealed no significant group differences on either night (Fig. 2A, third column).

We further examined the MPD for channel pairs that showed strong phase synchronization (PLV > 0.5; Fig. 2B). In the non-PTSD group (Fig. 2B, second column), the MPD values were within the range of −0.4 rad to 0.4 rad (−23° to 23°), indicating that the phase delays relative to the seed channel were less than 6 ms [=(23°/360°) × (1000/slow-spindle frequency)]. The PTSD group tended to show even smaller phase delays (Fig. 2B, first column). A statistical comparison between the PTSD and non-PTSD groups indicated that the MPD values between the frontal seed channel and the distributed centro-parietal channels for the PTSD group were smaller than those for the non-PTSD group (uncorrected $p < 0.05$). These differences were most prominent over the left centro-parietal area and consistent across nights (Fig. 2B, third column). However, none of the group differences survived the correction for multiple comparisons across channel pairs. The channel pair Fz−C5 showed the highest test-statistic value across the two nights, which approached significance after correction (Night 1: F-value = 8.2, uncorrected $p = 0.006$, corrected $p = 0.082$, Cohen's $d = -0.89$; Night 2: F-value = 7.9, uncorrected $p = 0.007$, corrected $p = 0.098$, Cohen's $d = -0.87$).

3.2.2. Results for fast spindles

Panels C and D in Fig. 2 show the topographical distributions of the PLV and the MPD, respectively, between the parietal seed channel Pz and all other channels for fast spindles. We observed no consistent group differences in either the PLV or the MPD across nights.

3.3. Replication analysis

The main finding of the discovery analysis was that, relative to the non-PTSD group, the PTSD group showed a smaller MPD between the frontal and centro-parietal channel pairs for slow spindles. In the replication analysis, we sought to assess whether this finding was reproducible in the remaining set of participants not used in the discovery analysis (13 PTSD and 18 non-PTSD).

Fig. 3A shows the topographical results for the discovery, replication, and combined sets. The topographical distributions from the

Table 1
Number of sleep spindles detected in the discovery and replication sets.

	Discovery set			Replication set		
	PTSD [n = 18] Mean (SD)	Non-PTSD [n = 29] Mean (SD)	Group comparison *p*-value	PTSD [n = 13] Mean (SD)	Non-PTSD [n = 18] Mean (SD)	Group comparison *p*-value
Number of slow spindles from channel Fz						
Whole night						
Night 1	1170 (410)	1178 (355)	0.793	1263 (360)	1384 (441)	0.238
Night 2	1202 (342)	1214 (321)	0.991	1267 (319)	1409 (333)	0.105
1st sleep cycle						
Night 1	412 (237)	446 (272)	0.784	363 (101)	490 (197)	0.057
Night 2	362 (192)	384 (259)	0.654	417 (164)	381 (175)	0.660
2nd sleep cycle						
Night 1	304 (93)	282 (123)	0.477	333 (108)	362 (153)	0.645
Night 2	316 (133)	330 (117)	0.622	350 (125)	406 (131)	0.238
3rd sleep cycle						
Night 1	236 (113)	231 (124)	0.818	279 (115)	251 (99)	0.873
Night 2	234 (82)	248 (91)	0.678	239 (106)	326 (119)	0.032*
Number of fast spindles from channel Pz						
Whole night						
Night 1	948 (526)	975 (405)	0.491	1066 (268)	1087 (400)	0.764
Night 2	990 (473)	1061 (391)	0.464	1126 (388)	1216 (374)	0.412
1st sleep cycle						
Night 1	270 (190)	294 (183)	0.477	287 (125)	269 (142)	0.459
Night 2	220 (148)	244 (131)	0.554	256 (109)	241 (120)	0.561
2nd sleep cycle						
Night 1	212 (110)	229 (119)	0.592	225 (97)	264 (149)	0.674
Night 2	244 (135)	261 (135)	0.793	297 (120)	290 (141)	0.826
3rd sleep cycle						
Night 1	230 (149)	211 (114)	0.694	235 (72)	233 (116)	0.734
Night 2	208 (102)	252 (116)	0.225	248 (121)	303 (143)	0.307

*$p < 0.05$, Wilcoxon rank-sum test.

replication analysis resembled the original ones; the group differences were most prominent over the left centro-parietal area and consistent across nights (Fig. 3A, second column). The number of significant (uncorrected $p < 0.05$) channel pairs in the replication analysis (6 pairs on both nights) was less than that in the discovery analysis (21 pairs on Night 1 and 22 pairs on Night 2). This may be partially due to the lower statistical power of the replication set, as its sample size was smaller than that of the discovery set. When we combined the discovery and replication sets (31 PTSD and 47 non-PTSD), the group differences passed the correction for multiple channel-pair comparisons (corrected $p < 0.05$; indicated by the white dots in Fig. 3A, third column). One channel pair (Fz–C5) on Night 1 and three channel pairs (Fz–C3, Fz–C5, and Fz–CP5) on Night 2 further passed the Bonferroni correction for the four metrics investigated ($p < 0.05/4 = 0.013$).

We further assessed the reproducibility of the results for the Fz–C5 channel pair, using the three tests discussed in the Materials and methods. We considered this channel pair to be of particular interest because it showed the highest value for the test statistic in the discovery analysis. In the replication analysis, the group difference in the MPD for this channel pair during slow spindles was in the same direction as it was in the discovery analysis, and was statistically significant for both Night 1 (uncorrected $p = 0.028$) and Night 2 (uncorrected $p = 0.020$) (Fig. 3B). The replication effect sizes (Night 1: Cohen's $d = -0.88$; Night 2: Cohen's $d = -0.94$) fell within the 95% CI of the original effect sizes (Fig. 3C). After combining the discovery and replication sets, the group differences remained statistically significant (uncorrected $p < 0.001$ for both nights). These results satisfied all three tests on both nights and, thereby, reproduced the original finding on the MPD during slow spindles in the replication set. However, the first test did not reach statistical significance after corrections for multiple comparisons. To be comprehensive, we also assessed the reproducibility of the findings for all channel pairs (N = 15) that were significant (uncorrected $p < 0.05$) on both nights in the discovery analysis (Supplementary Table S4). Of the 15 channel pairs, 14 passed at least two of the three tests on both nights, showing that our original findings tended to be reproducible.

We performed several additional analyses to assess the robustness and specificity of our findings. First, we examined whether the MPD findings obtained using a different frontal channel, F3 or F4, as the seed channel would yield similar results as those obtained using Fz as the seed channel. The overall trend in the findings remained the same (Supplementary Fig. S1). Second, to evaluate the robustness of our findings to variations in the method used to detect spindles, we re-analyzed our data using *1*) different spindle-detection thresholds (i.e., using the 92nd and 98th percentiles of the RMS amplitude, instead of the 95th percentile value) and *2*) a different spindle-detection algorithm (Ferrarelli et al., 2007). These changes did not alter our overall findings (Supplementary Fig. S2). Third, to test the specificity of our findings to spindle intervals, we analyzed the MPD in the slow-spindle frequency band during randomly selected non-spindle intervals (from N2 and N3 stages only). The group differences in the MPD were less prominent during non-spindle intervals than during spindle intervals (Supplementary Fig. S3). Fourth, we verified that the number of data points used for the PLV and MPD estimations did not differ between the PTSD and non-PTSD groups ($p > 0.05$), suggesting that this factor was not a potential bias. Finally, to investigate whether spurious phase synchronization affected our results, we created surrogate datasets and performed analysis using the method described in Lachaux et al. (1999) and Trujillo et al. (2005). Briefly, we created 1000 surrogate datasets by randomly shuffling the order of the analysis windows for the non-seed channels while keeping intact the original order of the analysis windows for the seed channel. Such surrogate datasets have similar energetic and temporal characteristics as the original dataset, but with disrupted time-dependency between the seed and non-seed channel pairs. For each surrogate dataset, we computed group-average PLV for each channel pair. To account for all comparisons across channel pairs, we selected the largest PLV of all channel pairs for each surrogate dataset and formed a distribution over the 1000 surrogates. The 95%

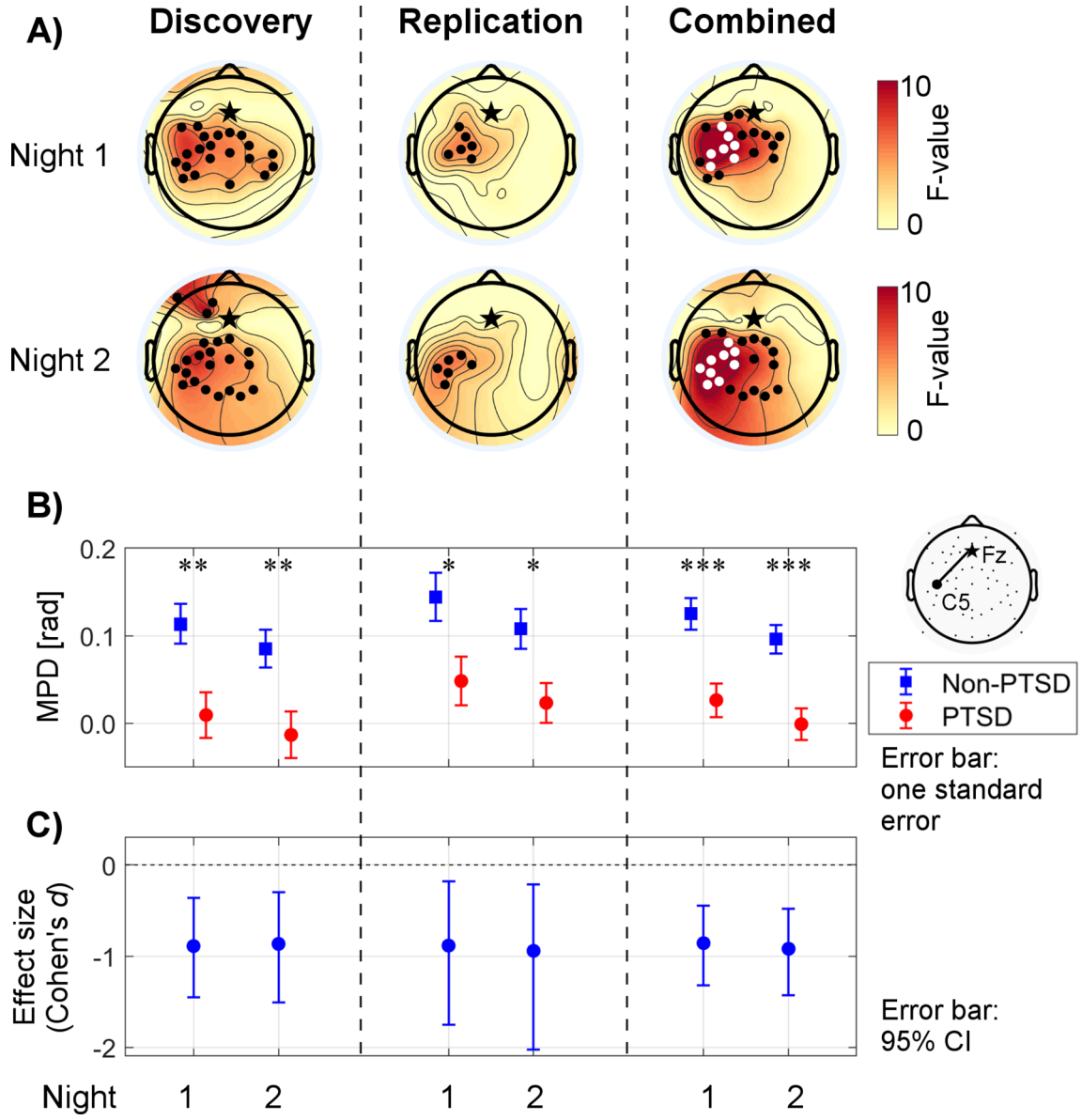

Fig. 3. Assessment of reproducibility. A) Topographical results of the mean phase difference (MPD) during slow spindles from the discovery (18 PTSD and 29 non-PTSD), replication (13 PTSD and 18 non-PTSD), and combined (31 PTSD and 47 non-PTSD) analyses. The heat maps show F-values of the statistical comparisons (Watson – Williams tests) between the PTSD and non-PTSD groups at individual channels. Black stars indicate the seed channel Fz. Black dots indicate channels with uncorrected *p*-values less than 0.05, whereas white dots indicate channels that were statistically significant ($p < 0.05$) after accounting for multiple comparisons across channels. B) Between-group differences of the MPD during slow spindles for the selected Fz–C5 channel pair in the discovery, replication, and combined analyses. The plotted values show group means, whereas the error bars indicate one standard error of the mean. Asterisks indicate levels of statistical significance for the group differences: $*p < 0.05$, $**p < 0.01$, $***p < 0.001$. C) Effect sizes of group differences of the MPD during slow spindles (for the Fz–C5 channel pair) in the discovery, replication, and combined analyses. Negative values indicate that the MPD was lower in the PTSD group than in the non-PTSD group. We used Cohen's *d* as the measure of effect size. Error bars indicate 95% confidence intervals (CIs) of the effect sizes; the horizontal dashed line indicates an effect size of zero. A 95% CI that does not cross zero implies that the effect is significant at the 0.05 level.

confidence interval of the corresponding distribution represents the level of spurious phase synchronization and can be used to test for the significance of the observed PLVs. For each of the two nights in both the PTSD group and the non-PTSD group, the mean and upper 95% confidence limit of the surrogate distributions were less or equal to 0.021 and 0.024, respectively (Supplementary Fig. S4). We verified that the obtained PLVs of all channel pairs in the original analysis exceeded the upper 95% confidence limit of the surrogate distribution, suggesting that the obtained phase dependencies were not due to random, coincidental synchronization.

3.4. Correlation with PTSD symptom severity

Based on the findings above, we performed an exploratory analysis to assess the correlation between the MPD during slow spindles and the severity of PTSD symptoms (as indicated by the CAPS scores), using the combined set. Table 2 summarizes the results. The MPD during slow spindles for the channel pair Fz – C5 was negatively correlated with the CAPS total and subscale scores across all participants, in each of the two nights ($p < 0.05$). When we restricted the analysis to participants with PTSD, none of the correlations were statistically significant. The MPD during slow spindles and the CAPS hyperarousal score showed a trend towards a negative correlation across participants with PTSD (Night 1:

Table 2
Correlations (Spearman's rho) between mean phase difference (MPD) during slow spindles for the Fz–C5 channel pair and the CAPS total and subscale scores.

	Total CAPS	Intrusion (CAPS-B)	Avoidance (CAPS-C)	Hyperarousal (CAPS-D)
Among all participants (n = 78)				
Night 1	−0.27*	−0.23*	−0.28*	−0.26*
Night 2	−0.34**	−0.30*	−0.38***	−0.34**
Among PTSD participants (n = 31)				
Night 1	−0.14	−0.02	0.00	−0.22
Night 2	−0.25	−0.14	−0.16	−0.33

CAPS, Clinician-Administered PTSD Scale; *$p < 0.05$; **$p < 0.01$; ***$p < 0.001$.

Spearman's rho = −0.22, $p = 0.226$; Night 2: Spearman's rho = −0.33, $p = 0.066$).

3.5. Group differences across sleep cycles

We also examined group differences in the MPD during slow spindles for the Fz–C5 channel pair across the first three sleep cycles, using the combined set (Fig. 4). A two-way rANOVA with group and sleep cycle as between- and within-subject factors, respectively, revealed a significant effect of group on the MPD during slow spindles (Night 1: F-value = 11.9, $p < 0.001$; Night 2: F-value = 16.6, $p < 0.001$), but no significant effect of sleep cycle (Night 1: F-value = 0.7, $p = 0.492$; Night 2: F-value = 1.4, $p = 0.241$) or group × sleep cycle interaction (Night 1: F-value = 0.7, $p = 0.496$; Night 2: F-value = 1.1, $p = 0.344$). These results indicate that the group differences in slow-spindle MPD were consistent across sleep cycles.

4. Discussion

Sleep spindles measured by EEG are highly synchronized across widespread scalp regions. Here, we aimed to investigate whether the synchronization patterns of spindles between EEG channels are altered in individuals with PTSD. We found that despite the absence of significant group differences in synchronization strength (as quantified by the PLV), synchronization delays (as quantified by the MPD) between the frontal and left centro-parietal channel pairs during slow spindles were smaller in the PTSD group than in the non-PTSD group. Notably, this effect was consistent across nights and the trend was reproducible across subsamples of our study population. When using the entire sample, the effect became statistically significant after correction for multiple comparisons. Our findings provide initial evidence that inter-channel phase differences during sleep spindles may be altered in Veterans with PTSD.

4.1. Implications of altered phase difference during sleep spindles

The widespread synchronization during sleep spindles is thought to be generated via reciprocal interactions between inhibitory thalamic reticular nucleus (TRN) neurons and excitatory thalamocortical (TC) neurons [see Luthi (2014) and Beenhakker and Huguenard (2009) for reviews]. Briefly, when a TRN neuron fires, it sends inhibitory signals to multiple TC neurons through its divergent projections. After a delay, the inhibited TC neurons undergo rebound excitation and send excitatory signals to the cortex and, en route, re-activate a larger number of TRN neurons to initiate the next cycle of inhibitory-excitatory oscillation. This interplay between inhibition and excitation increasingly recruits TRN and TC neurons into synchronized firing, which triggers rhythmic activity across a wide range of cortical areas. The thalamically triggered rhythm is further amplified within the cortical circuitry (Kandel and Buzsaki, 1997), contributing to the strongly synchronized spindle waves observed at the scalp level.

Hence, in theory, phase differences during spindles are attributed by many potential factors in the aforementioned processes, such as the speed of neural-signal propagation in the underlying thalamocortical circuits, the trajectories of the propagation, and the location of the neuronal groups that initiate spindles. The altered spindle-phase differences in PTSD may indicate pathological changes in one or more of these factors. Notably, it has been suggested that the propagation speed of spontaneous neural activity depends on the state of the network, with faster propagation occurring in the more active state (Wanger et al., 2013). If the reduced phase differences during spindles in PTSD observed in the current study were indeed caused by increased propagation speed, our finding could indicate that the underlying brain circuits in PTSD are abnormally active during NREM sleep. This is in agreement with the notion that hyperarousal is a primary symptom of PTSD (Woodward et al., 2000) that may persist during sleep (Wang et al., 2020a). Consistent with this interpretation, the phase difference during slow spindles tended to negatively correlate with the CAPS hyperarousal score across PTSD participants.

The spindle-phase differences we observed here were less than 0.4 rad, indicating that the propagation delays between two different recording sites were merely a few milliseconds (i.e., < 6 ms). Such near-simultaneous occurrence of spindles over different regions of the scalp is consistent with previous observations in animals using multisite

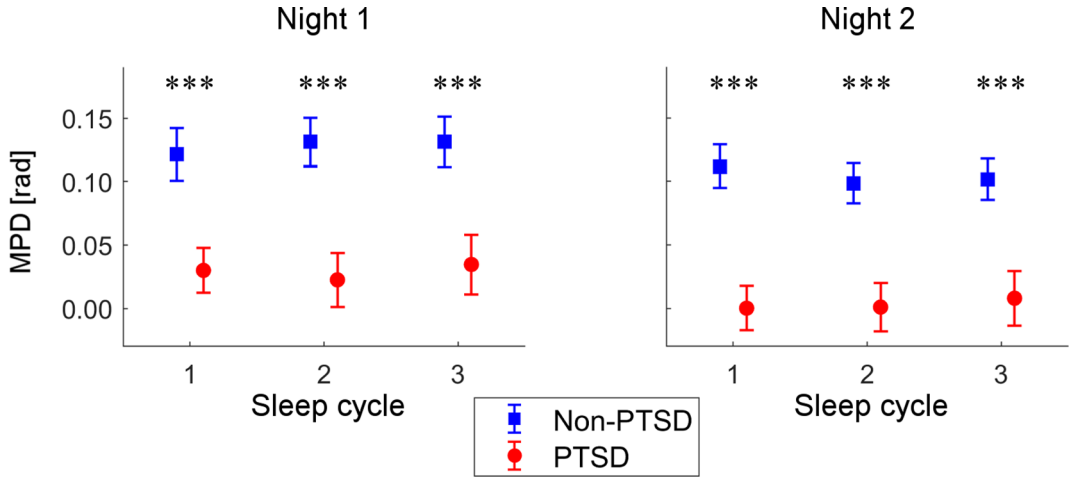

Fig. 4. Group differences in the mean phase difference (MPD) during slow spindles for the first 3 sleep cycles (Fz–C5 channel pair; combined set). Error bars indicate standard errors of the mean. Asterisks indicate the level of statistical significance for the group differences: ***$p < 0.001$.

cortical recordings (Contreras et al., 1997), but not with a more recent human scalp EEG study that reported spindle propagation delays of 8 to 28 ms between adjacent posterior-anterior electrodes (O'Reilly and Nielsen, 2014). This discrepancy may be attributed to differences in the computational methods used for assessing propagation delays. It is worth noting that volume conduction may contribute to the small phase delays observed in the present study, as mixing of source activities tends to attenuate the original phase difference (Robinson et al., 2008). Thus, the actual cortical-level phase differences during spindles may be larger than what we observed at the scalp level. Nevertheless, volume conduction cannot artificially generate non-zero phase delays (Stam et al., 2007) and, therefore, the observed delays, as small as they may be, are likely to reflect the true properties of the underlying networks.

Interestingly, we observed altered phase differences in subjects with PTSD during slow spindles but not during fast spindles. It has been suggested that different topographical projections between the thalamic nuclei and cortical regions could explain differences in spindle frequency (Andrillon et al., 2011; Cappe et al., 2009; Zhang et al., 2010). Specifically, it has been proposed that the ventral and anterior-dorsal nuclei mainly project themselves into the prefrontal regions of the brain and give rise to slow spindles, whereas the posterior and lateral-dorsal nuclei mainly project themselves into the centro-parietal regions and give rise to fast spindles. Hence, our findings suggest the possibility that pathological changes in PTSD may be specific to the prefrontal projections of the thalamocortical system.

4.2. Reproducibility of our findings

The altered phase differences during slow spindles in Veterans with PTSD tended to be reproducible. The effect sizes and uncorrected statistical significance were consistent across the two study nights and across subsamples of the study population. The consistency across nights indicates high test–retest reliability of spindle-phase relations. This is in agreement with and extends the notion that sleep-spindle characteristics are trait-like individual EEG attributes (De Gennaro et al., 2005, 2008). Such cross-night stability of spindles is in contrast to the considerable night-to-night variability of conventional sleep architecture parameters (Levendowski et al., 2009). Indeed, our spindle findings were stronger and more consistent than the trends we saw in the sleep architecture parameters (Supplementary Table S2). These results suggest that altered phase differences during spindles in PTSD may not be explained by changes in sleep macrostructure. In addition, the proposed PLV and MPD metrics untangled more reproducible results than standard sleep EEG microstructural metrics, such as the spectral power of sleep EEG at specific sleep stages (Wang et al., 2020a). It seems that brain connectivity patterns may better describe sleep disturbances in PTSD than previously reported power patterns.

The consistency across subsamples of the study population suggests that our discoveries are unlikely to be chance findings. In particular, Fig. 3 shows that the group differences were most prominent over the left centro-parietal region—a topographical pattern that was preserved in the replication analysis. We also attempted to assess the robustness of our findings by re-running our analyses using different channels as the seed channel and different methods to define spindle intervals. We found that our original findings held true for each of these attempts. We are unaware of any previous study that has examined the phase delay during spindles in PTSD or in any other psychiatric condition. As such, we have no frame of reference to discuss our observations in the context of other studies. However, the reproducibility and robustness of our findings invites future research to further investigate this discovery, and to explore many of the unknown aspects of spindle-phase differences, such as alterations in other medical conditions, responses to mental health treatments, variations with age and sex, and associations with sleep and cognitive functions.

4.3. Limitations

The sample used in our analyses consisted of only men. Although we had data from 7 women, 6 of them were in the PTSD group and only 1 was in the non-PTSD group. We therefore decided to exclude all women to prevent potential confounding due to an unbalanced sex ratio. The extent to which our findings are generalizable to women have yet to be determined. It is worth mentioning, nonetheless, that our findings held true even after we included the 7 women. Another limitation is that we assessed reproducibility by subdividing the data from the same study rather than by using data from a totally independent study. We cannot rule out the possibility that the reproducible findings observed here were due to certain unknown systematic biases in data recording and analysis. Future studies carried out by different research groups will make it possible to establish the consistency of the current findings.

4.4. Conclusions

In the present study, we discovered that the inter-channel phase differences during slow spindles were altered in individuals with PTSD. These alterations may reflect pathological changes in the underlying thalamocortical system. Notably, the findings were consistent across nights and reproducible across samples, suggesting that phase differences during sleep spindles may serve as a means to discriminate Veterans with PTSD. If independently confirmed, this EEG feature may prove useful in the objective diagnosis of PTSD, monitoring of its progression, assessment of treatment outcomes, and development of sleep-focused interventions. Our observations also open avenues for future research to decipher the functional relevance of spindle-phase differences and to explore how such differences relate to other sleep-associated disorders.

CRediT authorship contribution statement

Chao Wang: Conceptualization, Methodology, Software, Validation, Formal analysis, Writing - original draft, Visualization. **Srinivas Laxminarayan:** Software, Formal analysis. **J. David Cashmere:** Investigation, Data curation. **Anne Germain:** Conceptualization, Resources, Supervision. **Jaques Reifman:** Funding acquisition, Conceptualization, Methodology, Resources, Supervision, Project administration, Writing - review & editing, Methodology, Software, Validation, Formal analysis, Writing - original draft.

Acknowledgments

This work was sponsored by U.S. Defense Health Program (grant No. W81XWH-14-2-0145), managed by the U.S. Army Military Operational Medicine Program Area Directorate, Ft. Detrick, MD. The University of Pittsburgh Medical Center was also partially funded by the Clinical and Translational Science Institute at the University of Pittsburgh (UL1 TR001857).

Disclosures

This was not an industry-supported study. The authors have indicated no financial conflicts of interest. The opinions and assertions contained herein are the private views of the authors and are not to be construed as official or as reflecting the views of the U.S. Army, the U.S. Department of Defense, or The Henry M. Jackson Foundation for the Advancement of Military Medicine, Inc. This paper has been approved for public release with unlimited distribution.

Appendix A. Supplementary data

Supplementary data to this article can be found online at https://doi.org/10.1016/j.nicl.2020.102390.

References

Andrillon, T., Nir, Y., Staba, R.J., Ferrarelli, F., Cirelli, C., Tononi, G., Fried, I., 2011. Sleep spindles in humans: insights from intracranial EEG and unit recordings. J. Neurosci. 31, 17821–17834.

Astori, S., Wimmer, R.D., Luthi, A., 2013. Manipulating sleep spindles–expanding views on sleep, memory, and disease. Trends Neurosci. 36, 738–748.

Aydore, S., Pantazis, D., Leahy, R.M., 2013. A note on the phase locking value and its properties. Neuroimage 74, 231–244.

Bastien, C.H., Vallieres, A., Morin, C.M., 2001. Validation of the Insomnia Severity Index as an outcome measure for insomnia research. Sleep Med. 2, 297–307.

Beenhakker, M.P., Huguenard, J.R., 2009. Neurons that fire together also conspire together: is normal sleep circuitry hijacked to generate epilepsy? Neuron 62, 612–632.

Berens, P., 2009. CircStat: a MATLAB Toolbox for Circular Statistics. J. Stat. Softw. 31, 21.

Blake, D.D., Weathers, F.W., Nagy, L.M., Kaloupek, D.G., Gusman, F.D., Charney, D.S., Keane, T.M., 1995. The development of a Clinician-Administered PTSD Scale. J. Trauma. Stress 8, 75–90.

Bonjean, M., Baker, T., Bazhenov, M., Cash, S., Halgren, E., Sejnowski, T., 2012. Interactions between core and matrix thalamocortical projections in human sleep spindle synchronization. J. Neurosci. 32, 5250–5263.

Brunner, D.P., Vasko, R.C., Detka, C.S., Monahan, J.P., Reynolds 3rd, C.F., Kupfer, D.J., 1996. Muscle artifacts in the sleep EEG: automated detection and effect on all-night EEG power spectra. J. Sleep Res. 5, 155–164.

Buysse, D.J., Germain, A., Moul, D.E., Franzen, P.L., Brar, L.K., Fletcher, M.E., Begley, A., Houck, P.R., Mazumdar, S., Reynolds 3rd, C.F., Monk, T.H., 2011. Efficacy of brief behavioral treatment for chronic insomnia in older adults. Arch. Intern. Med. 171, 887–895.

Buysse, D.J., Reynolds 3rd, C.F., Monk, T.H., Berman, S.R., Kupfer, D.J., 1989. The Pittsburgh Sleep Quality Index: a new instrument for psychiatric practice and research. Psychiatry Res. 28, 193–213.

Cappe, C., Morel, A., Barone, P., Rouiller, E.M., 2009. The thalamocortical projection systems in primate: an anatomical support for multisensory and sensorimotor interplay. Cereb. Cortex 19, 2025–2037.

Contreras, D., Destexhe, A., Sejnowski, T.J., Steriade, M., 1997. Spatiotemporal patterns of spindle oscillations in cortex and thalamus. J. Neurosci. 17, 1179–1196.

Cox, R., Schapiro, A.C., Manoach, D.S., Stickgold, R., 2017. Individual differences in frequency and topography of slow and fast sleep spindles. Front. Hum. Neurosci. 11, 433.

De Gennaro, L., Ferrara, M., Vecchio, F., Curcio, G., Bertini, M., 2005. An electroencephalographic fingerprint of human sleep. Neuroimage 26, 114–122.

De Gennaro, L., Marzano, C., Fratello, F., Moroni, F., Pellicciari, M.C., Ferlazzo, F., Costa, S., Couyoumdjian, A., Curcio, G., Sforza, E., Malafosse, A., Finelli, L.A., Pasqualetti, P., Ferrara, M., Bertini, M., Rossini, P.M., 2008. The electroencephalographic fingerprint of sleep is genetically determined: a twin study. Ann. Neurol. 64, 455–460.

Delorme, A., Makeig, S., 2004. EEGLAB: an open source toolbox for analysis of single-trial EEG dynamics including independent component analysis. J. Neurosci. Methods 134, 9–21.

Doman, J., Detka, C., Hoffman, T., Kesicki, D., Monahan, J.P., Buysse, D.J., Reynolds 3rd, C.F., Coble, P.A., Matzzie, J., Kupfer, D.J., 1995. Automating the sleep laboratory: implementation and validation of digital recording and analysis. Int. J. Biomed. Comput. 38, 277–290.

Ferrarelli, F., Huber, R., Peterson, M.J., Massimini, M., Murphy, M., Riedner, B.A., Watson, A., Bria, P., Tononi, G., 2007. Reduced sleep spindle activity in schizophrenia patients. Am. J. Psychiatry 164, 483–492.

First, M.B., Spitzer, R.L., 1997. Structured Clinical Interview for DSM-IV AXIS I Disorders: SCID-I. Biometrics Research Department, New York.

Fogel, S.M., Smith, C.T., 2011. The function of the sleep spindle: a physiological index of intelligence and a mechanism for sleep-dependent memory consolidation. Neurosci. Biobehav. Rev. 35, 1154–1165.

Germain, A., 2013. Sleep disturbances as the hallmark of PTSD: where are we now? Am. J. Psychiatry 170, 372–382.

Johns, M.W., 1991. A new method for measuring daytime sleepiness: the Epworth sleepiness scale. Sleep 14, 540–545.

Kandel, A., Buzsaki, G., 1997. Cellular-synaptic generation of sleep spindles, spike-and-wave discharges, and evoked thalamocortical responses in the neocortex of the rat. J. Neurosci. 17, 6783–6797.

Kim, S.J., Lyoo, I.K., Lee, Y.S., Kim, J., Sim, M.E., Bae, S.J., Kim, H.J., Lee, J.Y., Jeong, D.U., 2007. Decreased cerebral blood flow of thalamus in PTSD patients as a strategy to reduce re-experience symptoms. Acta Psychiatr. Scand. 116, 145–153.

Kobayashi, I., Boarts, J.M., Delahanty, D.L., 2007. Polysomnographically measured sleep abnormalities in PTSD: a meta-analytic review. Psychophysiology 44, 660–669.

Lachaux, J.P., Rodriguez, E., Martinerie, J., Varela, F.J., 1999. Measuring phase synchrony in brain signals. Hum. Brain Mapp. 8, 194–208.

Lanius, R.A., Bluhm, R., Lanius, U., Pain, C., 2006. A review of neuroimaging studies in PTSD: heterogeneity of response to symptom provocation. J. Psychiatr. Res. 40, 709–729.

Lanius, R.A., Williamson, P.C., Bluhm, R.L., Densmore, M., Boksman, K., Neufeld, R.W., Gati, J.S., Menon, R.S., 2005. Functional connectivity of dissociative responses in posttraumatic stress disorder: a functional magnetic resonance imaging investigation. Biol. Psychiatry 57, 873–884.

Laxminarayan, S., Wang, C., Ramakrishnan, S., Oyama, T., Cashmere, J.D., Germain, A., Reifman, J., 2020. Alterations in sleep EEG synchrony in combat-exposed veterans with PTSD. Sleep (in press). https://doi.org/10.1093/sleep/zsaa006.

Levendowski, D.J., Zack, N., Rao, S., Wong, K., Gendreau, M., Kranzler, J., Zavora, T., Westbrook, P.R., 2009. Assessment of the test-retest reliability of laboratory polysomnography. Sleep Breath 13, 163–167.

Liu, J., Ramakrishnan, S., Laxminarayan, S., Neal, M., Cashmere, D.J., Germain, A., Reifman, J., 2018. Effects of signal artefacts on electroencephalography spectral power during sleep: quantifying the effectiveness of automated artefact-rejection algorithms. J. Sleep Res. 27, 98–102.

Lowe, B., Kroenke, K., Herzog, W., Grafe, K., 2004. Measuring depression outcome with a brief self-report instrument: sensitivity to change of the Patient Health Questionnaire (PHQ-9). J. Affect. Disord. 81, 61–66.

Lustenberger, C., Wehrle, F., Tushaus, L., Achermann, P., Huber, R., 2015. The multidimensional aspects of sleep spindles and their relationship to word-pair memory consolidation. Sleep 38, 1093–1103.

Luthi, A., 2014. Sleep spindles: where they come from, what they do. Neuroscientist 20, 243–256.

Martin, N., Lafortune, M., Godbout, J., Barakat, M., Robillard, R., Poirier, G., Bastien, C., Carrier, J., 2013. Topography of age-related changes in sleep spindles. Neurobiol. Aging 34, 468–476.

Mellman, T.A., Hipolito, M.M., 2006. Sleep disturbances in the aftermath of trauma and posttraumatic stress disorder. CNS Spectr. 11, 611–615.

Neylan, T.C., Marmar, C.R., Metzler, T.J., Weiss, D.S., Zatzick, D.F., Delucchi, K.L., Wu, R.M., Schoenfeld, F.B., 1998. Sleep disturbances in the Vietnam generation: findings from a nationally representative sample of male Vietnam veterans. Am. J. Psychiatry 155, 929–933.

Nichols, T.E., Holmes, A.P., 2002. Nonparametric permutation tests for functional neuroimaging: a primer with examples. Hum. Brain Mapp. 15, 1–25.

O'Reilly, C., Nielsen, T., 2014. Assessing EEG sleep spindle propagation. Part 2: experimental characterization. J. Neurosci. Methods 221, 215–227.

Open Science, C., 2015. PSYCHOLOGY. Estimating the reproducibility of psychological science. Science 349, aac4716.

Robinson, P.A., Chen, P.C., Yang, L., 2008. Physiologically based calculation of steady-state evoked potentials and cortical wave velocities. Biol. Cybern. 98, 1–10.

Rosenblum, M., Kurths, J., 1998. Analysing synchronization phenomena from bivariate data by means of the Hilbert transform. In: Kantz, H., Kurths, J., Mayer-Kress, G. (Eds.), Nonlinear Analysis of Physiological Data. Springer, Berlin Heidelberg, Berlin, Heidelberg, pp. 91–99.

Stam, C.J., Nolte, G., Daffertshofer, A., 2007. Phase lag index: assessment of functional connectivity from multi channel EEG and MEG with diminished bias from common sources. Hum. Brain Mapp. 28, 1178–1193.

Suarez-Jimenez, B., Albajes-Eizagirre, A., Lazarov, A., Zhu, X., Harrison, B.J., Radua, J., Neria, Y., Fullana, M.A., 2019. Neural signatures of conditioning, extinction learning, and extinction recall in posttraumatic stress disorder: a meta-analysis of functional magnetic resonance imaging studies. Psychol. Med. 1, 1–10.

Terpou, B.A., Densmore, M., Theberge, J., Frewen, P., McKinnon, M.C., Lanius, R.A., 2018. Resting-state pulvinar-posterior parietal decoupling in PTSD and its dissociative subtype. Hum. Brain Mapp. 39, 4228–4240.

Thatcher, R.W., 2012. Coherence, phase differences, phase shift, and phase lock in EEG/ERP analyses. Dev. Neuropsychol. 37, 476–496.

Thatcher, R.W., North, D.M., Biver, C.J., 2008. Development of cortical connections as measured by EEG coherence and phase delays. Hum. Brain Mapp. 29, 1400–1415.

Trujillo, L.T., Peterson, M.A., Kaszniak, A.W., Allen, J.J., 2005. EEG phase synchrony differences across visual perception conditions may depend on recording and analysis methods. Clin. Neurophysiol. 116, 172–189.

Varela, F., Lachaux, J.P., Rodriguez, E., Martinerie, J., 2001. The brainweb: phase synchronization and large-scale integration. Nat. Rev. Neurosci. 2, 229–239.

Wang, C., Ramakrishnan, S., Laxminarayan, S., Dovzhenok, A., Cashmere, J.D., Germain, A., Reifman, J., 2020a. An attempt to identify reproducible high-density EEG markers of PTSD during sleep. Sleep 43 (1). https://doi.org/10.1093/sleep/zsz207.

Wang, C., Ramakrishnan, S., Laxminarayan, S., Dovzhenok, A., Cashmere, J.D., Germain, A., Reifman, J., 2020b. Increased oscillatory frequency of sleep spindles in combat-exposed veteran men with post-traumatic stress disorder. Sleep (in press). https://doi.org/10.1093/sleep/zsaa064.

Wanger, T., Takagaki, K., Lippert, M.T., Goldschmidt, J., Ohl, F.W., 2013. Wave propagation of cortical population activity under urethane anesthesia is state dependent. BMC Neurosci. 14, 78.

Warby, S.C., Wendt, S.L., Welinder, P., Munk, E.G., Carrillo, O., Sorensen, H.B., Jennum, P., Peppard, P.E., Perona, P., Mignot, E., 2014. Sleep-spindle detection: crowdsourcing and evaluating performance of experts, non-experts and automated methods. Nat. Methods 11, 385–392.

Woodward, S.H., Murburg, M.M., Bliwise, D.L., 2000. PTSD-related hyperarousal assessed during sleep. Physiol. Behav. 70, 197–203.

Yin, Y., Jin, C., Hu, X., Duan, L., Li, Z., Song, M., Chen, H., Feng, B., Jiang, T., Jin, H., Wong, C., Gong, Q., Li, L., 2011. Altered resting-state functional connectivity of thalamus in earthquake-induced posttraumatic stress disorder: a functional magnetic resonance imaging study. Brain Res. 1411, 98–107.

Zhang, D., Snyder, A.Z., Shimony, J.S., Fox, M.D., Raichle, M.E., 2010. Noninvasive functional and structural connectivity mapping of the human thalamocortical system. Cereb. Cortex 20, 1187–1194.